

# On the Measurement of Power Law Creep Parameters from Instrumented Indentation

P. SUDHARSHAN PHANI<sup>1,4</sup>, W.C. OLIVER,<sup>2</sup> and G.M. PHARR<sup>3</sup>

1.—International Advanced Research Centre for Powder Metallurgy and New Materials (ARCI), Balapur PO, Hyderabad, Telangana 500005, India. 2.—Nanomechanics Inc., 105 Meco Ln, Oak Ridge, TN 37830-7263, USA. 3.—Department of Materials Science and Engineering, Texas A&M University, College Station, TX 77843-3003, USA. 4.—e-mail: spphani@yahoo.com

Recently the measurement of the creep response of materials at small scales has received renewed interest largely because the equipment required to perform high-temperature nanomechanical testing has become available to an increasing number of researchers. Despite that increased access, there remain several significant experimental and modeling challenges in small-scale mechanical testing at elevated temperatures that are as yet unresolved. In this regard, relating the creep response observed with high-temperature instrumented indentation experiments to macroscopic uniaxial creep response is of great practical value. In this review, we present an overview of various methods currently being used to measure creep with instrumented indentation, with a focus on geometrically self-similar indenters, and their relative merits and demerits from an experimental perspective. A comparison of the various methods to use those instrumented indentation results to predict the uniaxial power law creep response of a wide range of materials will be presented to assess their validity.

## INTRODUCTION

As the size of engineering components continues to decrease, there has been an associated interest in understanding the material response at small scales. This has renewed the interest in mechanical property measurements at small scales where many of the conventional testing methods may not be either directly applicable or feasible—thin films, MEMS devices and many surface engineered components are a few examples. In such cases, indentation-based testing is an excellent option, given that it is fairly simple, quick, relatively inexpensive, and consumes very little material, which usually results in a larger number of tests being carried out leading to better statistics. Nevertheless, unlike uniaxial compression/tension testing wherein the stress fields are uniform, the stress fields developed during indentation are very complex and pose a challenge in data analysis. In addition, the uniaxial creep response is of primary interest to the small-scale mechanics community for modeling and design.

For these reasons, there is great value in estimating uniaxial creep parameters by indentation testing. It is well known that the measured strength

of a material often depends on strain, strain rate, temperature, sample size (test volume), and microstructure. Of these, the quasi-static room temperature uniaxial stress–strain response is of primary interest. There have been several attempts<sup>1–7</sup> to extract the equivalent uniaxial stress–strain response from indentation, and this area is still actively being researched. Similarly, there has been a great deal of interest in the measurement of time-dependent plastic properties at small scales, especially in the electronics packaging industry for studying the creep response of solder materials<sup>8,9</sup> and high-temperature creep of thermal barrier coatings<sup>10</sup> where conventional testing techniques are not feasible. In these cases, the additional complication of testing under nonambient conditions/elevated temperatures, in turn, poses several challenges in instrument design and measurement.<sup>11–13</sup> Recent advances in electronics and instrument design have resulted in many high-temperature instrumented indentation systems being commercially available,<sup>11,14</sup> which has renewed the interest in measurement of strain rate and temperature-dependent hardness or strength at small scales.

This review presents an overview of currently available experimental methods to predict uniaxial power-law creep parameters from instrumented indentation with specific focus on geometrically self-similar indenters and metallic materials. The ability of current methods to accurately predict the uniaxial creep response from indentation testing for a wide range of materials will be assessed. The interplay of indentation size effect, strain rate effects, and temperature effects and their influence on indentation creep measurements will also be discussed.

## INSTRUMENTED INDENTATION CREEP TESTING

In this section, we describe the different methods used for studying instrumented indentation creep and present their relative merits and demerits from a theoretical and experimental perspective. As mentioned earlier, we will limit the discussion to instrumented indentation with geometrically self-similar indenters and will not cover impression creep,<sup>15,16</sup> hot hardness,<sup>17–19</sup> and spherical indentation creep studies.<sup>20,21</sup> We note here that although many creep studies focus on steady-state conditions, some of the data described herein is most likely not steady state. The results and procedures described have been applied without judging if the data represents steady state or not.

Instrumented indentation creep and strain rate sensitivity testing can be performed in several different ways, viz., constant strain rate (CSR), strain rate jump (SRJ), constant load and hold (CLH), constant rate of loading (CRL), and step load tests.<sup>12,22–26</sup> Figure 1 shows a schematic of the load-time histories for the different methods (except step load tests) to measure the strain rate dependence of hardness. One technique used to approximate a constant strain rate test (CSR) for a geometrically self-similar indenter involves an exponential load-time history such that the ratio of loading rate to load ( $\dot{P}/P$ ) is a constant. For a material whose hardness and modulus are constant with depth, this should result in a constant ratio of the indenter velocity to the indentation depth ( $\dot{h}/h$ ), which is one of the definitions used for the indentation strain rate. While each CSR experiment enables measurement of hardness only at a single value of strain rate, this method could be useful to study materials that exhibit strain rate history dependent creep. The CSR test also provides a clear indication of indentation size effects if they exist in a given material.

Alternatively, a strain rate jump test (SRJ) can be performed, wherein multiple strain rates can be accessed in a single experiment by modifying the load-time history of a CSR test such that a different constant value of  $\dot{P}/P$  is maintained during different parts (depths) of the experiment. While this enables

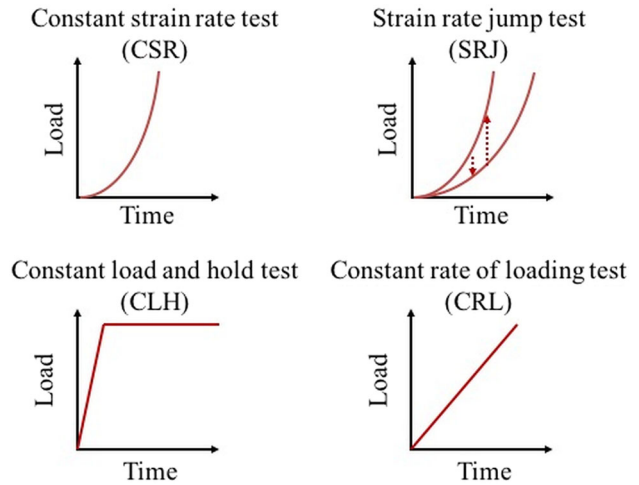


Fig. 1. Schematic of various methods to measure instrumented indentation creep.

access to multiple strain rates in a single experiment, it is difficult to perform and is prone to errors for many materials that exhibit depth dependent hardness for reasons other than strain rate effects, for example, an indentation size effect (ISE).<sup>27</sup> For instance, Fig. 2 shows the indentation strain rate ( $\dot{h}/h$ ) and hardness as a function of depth during CSR and SRJ tests on 1100 Al at 400°C from Phani and Oliver.<sup>12</sup> Figure 2a shows that the indentation strain rate was mostly constant for the CSR tests over the range of depth shown as was the temperature. In addition, any transients associated with tip imperfections are usually exhausted by 500 nm of depth. Hence, the observed dependence of the hardness on depth in the CSR tests is a real material effect. This indicates that there is some other mechanism resulting in a change in hardness as a function of depth as shown in Fig. 2b. They showed that such depth dependent hardness effects can result in inaccuracies in the measurement of strain rate effects during a SRJ test as evident from the plot where the change in hardness due to strain rate jump is comparable to change in hardness due to other mechanisms. In addition, the range of strain rates accessible by CSR or SRJ tests is limited to 0.5 1/s at the higher end due to instrumentation limitations.

The limitations of the SRJ and CSR tests associated with the wide range of depths required can be mitigated by choosing an experiment that uses a narrower range of depth. The constant load and hold test (CLH), wherein a constant load is maintained on the sample after a brief load ramp to the prescribed value, enables access to a wide range of strain rates in a single experiment, but the percentage change in depth during the hold is typically smaller than the range of depths used in the CSR or SRJ tests. The loading rate used should be chosen with the dynamics of the instrument in mind to avoid significant inertial effects at the end of the

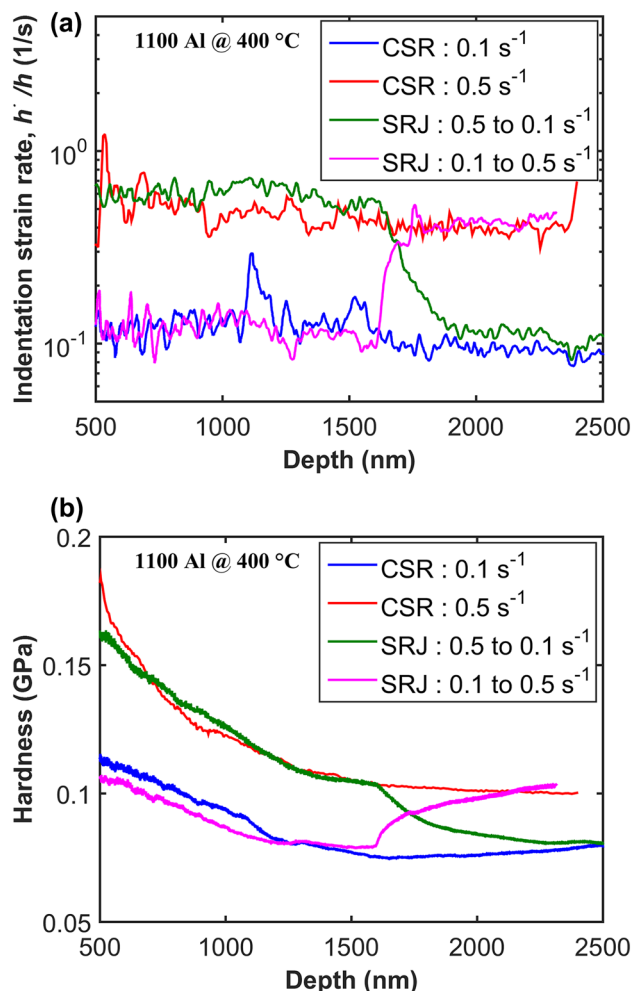


Fig. 2. (a) Indentation strain rate and (b) hardness as a function of depth during constant strain rate (CSR) and strain rate jump (SRJ) tests in 1100 Al at 400°C, showing the relative contributions of the strain rate effects and indentation size effect (Data from Ref. 12).

ramp. In addition, this method is specifically suitable for materials that exhibit depth dependent hardness as the contact depth does not change much in the hold segment compared to the depth at the beginning of the hold. The constant rate of loading test (CRL) where a constant loading rate,  $\dot{P}$ , is maintained is similar to the CLH test with regard to accessing a wide range of strain rates in a single experiment. Nevertheless, it is prone to errors for materials that exhibit depth dependent hardness as the contact depth can change significantly in the process of accessing different strain rates. Finally, the step load test involves ramping the force to a prescribed value as fast as the actuators can physically accomplish the change. This results in sweeping across a wide range of strain rates especially in the high strain rate regime ( $\sim 4000 \text{ 1/s}$ ).<sup>28</sup> Unlike the other methods, due to the fast loading, there are significant inertial effects, and accurately accounting for the instrument's dynamic contribution and time constants of the measurement signals

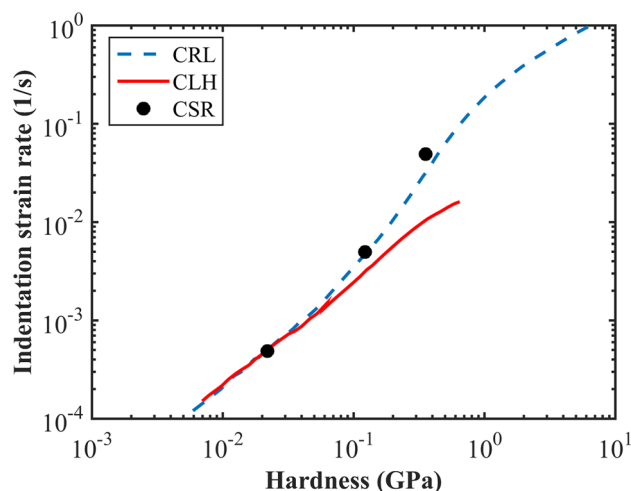


Fig. 3. Comparison of indentation strain rate versus hardness measured on amorphous selenium at 35°C for CLH (1 mN), CRL (0.1 mN/s), and CSR tests from Su et al.<sup>29</sup>

is critical for meaningful measurements. These are beyond the scope of the current review where we focus on the low-strain rate regime.

Given the various methods available to measure the indentation creep response, it is instructive to compare the indentation creep response measured by the different methods. Figure 3 shows a comparison of the indentation creep response of amorphous selenium measured at 35°C from CLH (1 mN), CRL (0.1 mN/s), and CSR tests, using a Berkovich indenter.<sup>29</sup> The data show good agreement between the various methods at lower strain rates while there is less agreement at higher strain rates and/or stresses. The authors suggest that this may be due to several effects such as elastic transients, power law breakdown, load-time history dependence, and non-steady-state response. Shen et al.<sup>30</sup> and Martinez et al.<sup>31</sup> have carried out a similar study wherein they compared the CSR and CLH tests on tin and single crystal aluminum and found that CLH tests were less repeatable compared to the CSR tests. While the drift during the long hold periods of a CLH test could be a potential issue, the transition from the initial load ramp to the hold segment results in a transient response causing inaccuracies in the measurements, especially for materials that show history dependence. This aspect has also been studied by other authors,<sup>32,33</sup> who have suggested that the primary creep results in a transient response during the initial part of the hold segment of a CLH test and suggested using a large indenter, high load, slow load ramp, and long hold periods to improve the accuracy of the CLH tests. Nevertheless, it is not entirely clear how much of the observed effect is due to instrument issues such as measurement time constants versus material properties. In addition, the performance of long durations tests is always compromised due to the drift in the displacement signal. Phani and Oliver<sup>12</sup> have

shown that with a fast response displacement sensor, short duration CLH tests can be performed to get accurate data from CLH tests for materials that do not show some of the effects mentioned earlier. For materials where long duration CLH tests are needed, Maier et al.<sup>34</sup> have proposed a new method that uses the dynamic contact stiffness ( $S$ ), instead of the displacement signal, which is very much less affected by thermal drift, to calculate the contact area and strain rate. While this method has a clear advantage over the conventional method that uses the displacement signal, the dynamic contact stiffness measurement capability does not exist in the basic version of many commercially available instrumented indenters.

Although the mentioned methods are fairly straightforward to implement at room temperature, performing these experiments at elevated temperatures poses several challenges. Of these, maintaining thermal equilibrium between the tip and sample during testing, minimizing and/or accurately determining thermal drift, and minimizing the influence of a depth dependent hardness are some of the important factors that can influence the indentation creep measurement. The choice of a suitable indenter tip material to minimize failure due to chemical reactions and accelerated wear and the associated corrections for their elastic deflections at elevated temperatures is an additional consideration in high-temperature testing. A detailed discussion of the various aspects of high-temperature nanomechanical testing instrumentation and testing strategies is presented in the review article of Wheeler et al.<sup>11</sup> and Phani and Oliver.<sup>12</sup> In view of these challenges and the relative merits of the various methods described, short duration CLH tests with fast response displacement sensors have significant advantages over the other methods in terms of accessing a wide range of strain rates in a single experiment, minimizing the influence of a depth dependent hardness and thermal drift. Nevertheless, proper care must be taken in interpreting these results in the initial part of the hold segment and assuring that they are not influenced by transients.

### EXTRACTION OF UNIAXIAL CREEP RESPONSE FROM INDENTATION

In this section, we present the basic ideas suggested by various researchers to extract the uniaxial creep response from instrumented indentation. For a power law creeping solid, the uniaxial steady-state strain rate ( $\dot{\epsilon}$ ) and uniaxial stress ( $\sigma$ ) are related through:

$$\dot{\epsilon} = \alpha \sigma^n \quad (1)$$

where  $n$  is the power law creep exponent and  $\alpha$  is a coefficient that depends on the activation energy, temperature, and microstructure. While normally used to describe steady-state creep behavior, we will assume that this equation can be used to fit non-

steady-state data as well. A similar equation for the case of indentation with geometrically self-similar indenters is:<sup>29</sup>

$$\dot{\epsilon}_i = \frac{\dot{h}}{h} = \beta p^n \quad (2)$$

where  $\dot{\epsilon}_i$  is the indentation strain rate,  $p$  is the hardness or contact pressure (load/contact area), and  $\beta$  is the indentation creep coefficient. Note that the power law exponent,  $n$ , is found to be identical for uniaxial and indentation testing under steady-state conditions.<sup>35</sup> As mentioned earlier, the uniaxial creep response is of interest to the community, and hence, determining the uniaxial creep response from the basic instrumented indentation creep measurements such as time ( $t$ ), indentation depth ( $h$ ), and load ( $P$ ) is of prime importance. This involves estimating the power law exponent  $n$  and the uniaxial creep coefficient  $\alpha$  or the uniaxial equivalent strain rate and stress from indentation strain rate and contact pressure (or hardness). The power law exponent  $n$  can be determined from the slope of the  $\log h$  versus  $\log t$  plot for the CLH and CRL tests and from the slope of the indentation strain rate versus contact pressure (or hardness) for the CSR tests.<sup>29</sup> While it is relatively straightforward to determine the power law exponent  $n$ , calculating  $\alpha$  requires additional inputs about the geometry of the contact (pile-up/sink-in) and indentation constraint factor. This has been done either by numerical analysis<sup>19,30,31,36–44</sup> or through a theoretical analysis,<sup>29,35</sup> which will be briefly summarized here. Both these approaches, assume steady-state, load-time history independent, power law creep behavior. Irrespective of the approach, they involve determining multiplicative factors ( $C_1$  and  $C_2$ ) to obtain the uniaxial equivalent strain rate and stress from indentation strain and contact pressure through the relations:

$$\sigma = C_1 p \quad \text{and} \quad \dot{\epsilon} = C_2 \dot{\epsilon}_i \quad (3)$$

From the factors  $C_1$  and  $C_2$ , the uniaxial creep coefficient,  $\alpha$ , can be calculated.

The methods, based on numerical analysis, mostly involve performing finite element analysis of indentation creep and determining a set of conversion factors to determine the uniaxial equivalent response from the indentation data.<sup>19,30,31,36–44</sup> This approach is not always easy to implement due to the need to perform finite element analysis (FEA). Nonetheless, based on FEA and dimensional analysis, Takagi et al.<sup>39</sup> have proposed that  $C_1 = 0.33$  and  $C_2 = 0.2$  for stress exponents in the range of 2–7 for a 68° cone. Similarly, Martinez et al.<sup>31</sup> have proposed that  $C_1 = 0.33$  and  $C_2 = 0.33$  for stress exponents in the range of 7–10 for a 70° cone. The stress conversion factor,  $C_1$  (0.33), was obtained by assuming that the constraint factor in indentation is 3. This is in contrast to the analysis of Bower et al.<sup>35</sup> who

showed that the conversion factors are a function of stress exponent and cone angle, which will be discussed next.

The alternative approach is the experimental method proposed by Su et al.<sup>29</sup> based on the theoretical analysis of Bower et al.<sup>35</sup> Bower et al.<sup>35</sup> proposed that the strain rate conversion factor ( $C_2$ ) is  $(1/c \tan(\theta))$  where  $c$  is the pile-up/sink-in parameter and the stress conversion factor  $C_1$ , which they denote by the variable  $F$ , are functions of the stress exponent and cone angle. Su et al.<sup>29</sup> performed finite element analysis for different cone angles and determined the functional dependence of  $c$  and  $F$  on the stress exponent and cone angle. Figure 4a and b show the comparison of the conversion factors  $C_1$  and  $C_2$  proposed by Su et al.<sup>29</sup> for 68° and 70° cone angles along with the conversion factors proposed by Takagi et al.<sup>39</sup> and Martinez et al.<sup>31</sup> The stress conversion factor ( $C_1$ ) proposed by Su et al.<sup>29</sup> varies with  $n$  while the other authors use a fixed value of 0.33 that is based on a simple assumption that the constraint factor in indentation is 3. Su et al.'s<sup>29</sup> stress conversion factor is almost a constant ( $\sim 0.36$ ) for stress exponent greater than 4. In the case of strain rate conversion factors, there is a clear effect of cone angle as per Su et al.'s<sup>29</sup> predictions. Nevertheless, even in this case, the conversion factor reaches a constant value at higher stress exponents ( $\sim 0.28$  and  $0.31$  for 70° and 68° cone, respectively). We will now assess the accuracy of the various conversion factors for a wide range of materials. We choose to use the conversion factors from Su et al.<sup>29</sup> that is valid for any stress exponent and Takagi et al.<sup>39</sup> ( $n = 2-7$ ) for comparison. While the simple analysis discussed here is for bulk, homogeneous, semi-infinite solids, it can be extended to more complicated sample geometries like 1D, 2D, or 3D structures and the corresponding conversion factors have to be determined accordingly.

Figure 5 shows a comparison of the uniaxial creep data and the uniaxial equivalent response calculated from indentation testing using different conversion factors for a wide range of stress exponents ranging from 1 to 8. The hardness and indentation strain rate are also plotted to demonstrate the magnitude of shift in the conversion process. Here we consider the cases where the mean pressure was independent of depth. For the case of amorphous selenium (Fig. 5a) tested at 35°C, which has a low stress exponent of 1.12, the conversion factors determined by Su et al.<sup>29</sup> result in extremely good agreement with the uniaxial data. For this stress exponent, the conversion factors from other groups are not available. Similarly, for the case of Al-Mg alloy (Fig. 5b), which has a stress exponent of 3.3, there is good agreement between the uniaxial data<sup>45</sup> and the uniaxial response calculated from indentation<sup>39</sup> using the different conversion factors. Similar results are found for the other cases, spanning a wide range of stress exponents, viz., 99.99% Al<sup>39,46</sup>

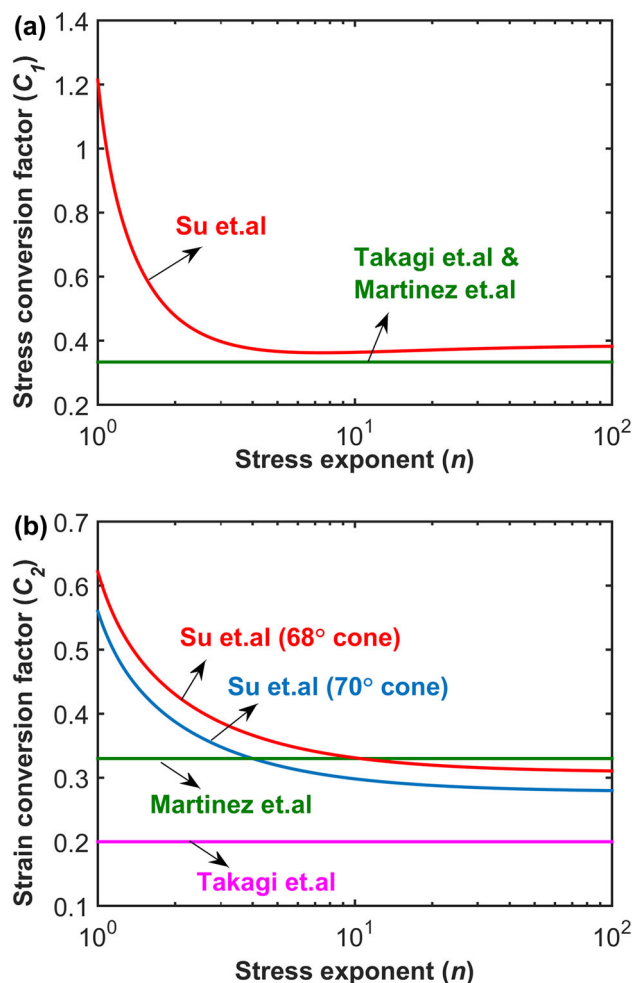


Fig. 4. Comparison of the conversion factors, (a)  $C_1$  and (b)  $C_2$  proposed by various authors.<sup>31,39</sup> The data for Su et al.<sup>29</sup> is calculated based on the equations provided in their work.

( $n = 4.9$ ) (Fig. 5c), 99.99% Al<sup>39,47</sup> ( $n = 6.9$ ) (Fig. 5d), and 1100 Al<sup>12,48</sup> ( $n = 7.7$ ) (Fig. 5e). The uniaxial response calculated using the different conversion factors are fairly close, especially at higher stress exponents, as may be expected from the closeness in the different conversion factors shown in Fig. 4. This clearly demonstrates the capability of the current approach, especially that of Su et al.<sup>29</sup> which can be used at any stress exponent, to determine the uniaxial creep response from indentation testing within the limits of the assumptions of the method. This result is very encouraging and to an extent surprising since the assumptions needed to model the relations between uniaxial and indentation creep, e.g., history independent behavior and no transient deformation, are most likely too oversimplified.

In addition to determining the uniaxial strain rate and stress, the activation energy for the corresponding creep mechanism has also been successfully determined from indentation studies.<sup>12,17,23,36,37,39</sup> This is calculated from the slope

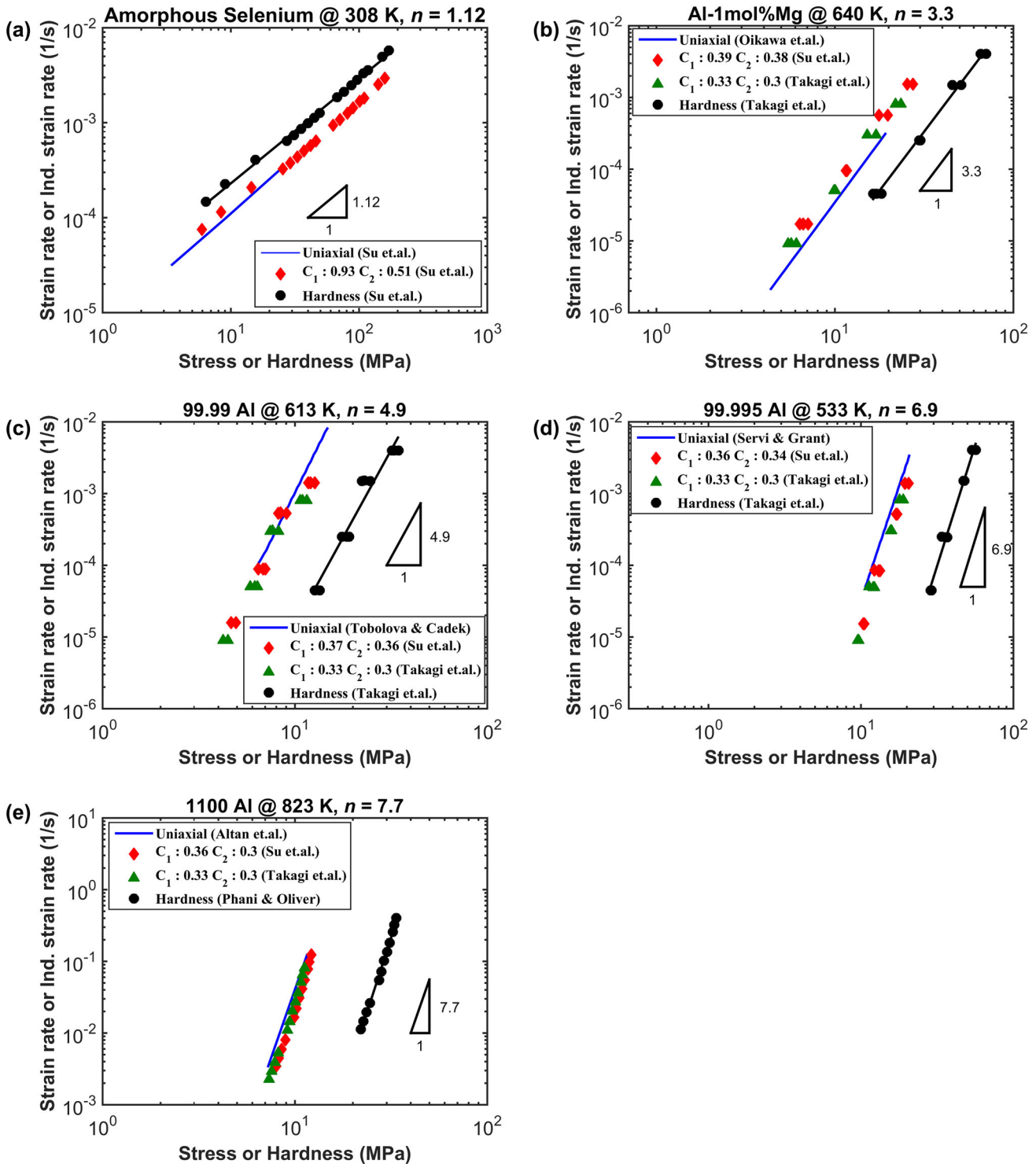


Fig. 5. Comparison of uniaxial creep data and the uniaxial equivalent response calculated from indentation testing using different conversion factors for a wide range of stress exponents from 1 to 8. (a) Amorphous selenium,<sup>29</sup> (b) Al-1 mol.%Mg,<sup>39,45</sup> (c) 99.99% Al,<sup>39,46</sup> (d) 99.995% Al,<sup>39,47</sup> and (e) 1100 Al.<sup>12,48</sup>

of the natural logarithm of strain rate and  $1/T$  at a constant value of hardness (stress) and is often found to correspond to the activation energy for self-diffusion.<sup>12,17,22,37,49</sup> The estimation of the activation energy helps in calculating the temperature

compensated strain rate to enable comparison of creep data over a wide range of temperatures and strain rates<sup>50</sup> as demonstrated by Phani and Oliver<sup>12</sup> for 1100 Al in Fig. 6, wherein, the temperature compensated uniaxial strain rate and

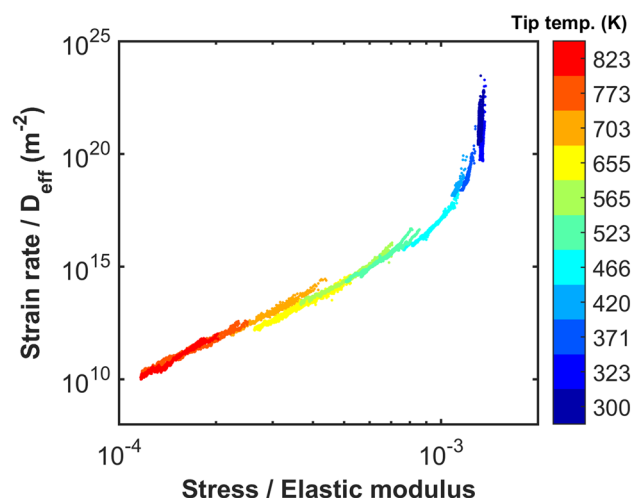


Fig. 6. Temperature compensated uniaxial strain rate versus normalized stress for 1100 Al from Phani and Oliver,<sup>12</sup> showing the convergence of indentation creep data measured at different temperatures onto a single curve.

modulus compensated stress calculated from the indentation data at different temperatures lie on a single curve. This further reinforces the capability of the currently available methods to predict uniaxial creep response from indentation.

While the capabilities of the current approach to determine uniaxial creep response from indentation are apparent from Fig. 5, it is important to recognize the strain requirement for achieving steady-state creep-like conditions during indentation testing. As indentation testing with a self-similar indenter induces a fixed value of representative strain, it may not always be possible to determine whether steady-state creep-like conditions are achievable at that value of strain and test temperature. Figure 7 shows the comparison of uniaxial creep data at two different values of strain for 1100 Al and Pb-In. The uniaxial equivalent response determined from indentation for 1100 Al<sup>12</sup> and Pb-In<sup>23</sup> are also shown. For the case of 1100 Al shown in Fig. 7a, the uniaxial data at 10% strain and 70% strain do not match at lower temperatures, which represent higher temperature compensated strain rates. For the case of Pb-In, the uniaxial creep data at 10% strain and 80% strain are very different due to strain softening.<sup>23</sup> Nevertheless, it is interesting to note that in both the cases, the data calculated from indentation creep testing using a Berkovich indenter, which is typically thought of as inducing ~8% representative strain, is close to the uniaxial response at 10%. This is not entirely surprising as the concept of representative strain is based on determining the strain at which the ratio of hardness to constraint factor matches the flow stress. While this is encouraging, it is important to recognize that both the uniaxial and the indentation data at 8% or 10% strain does not reflect a true steady-state creep response for these materials at the test temperatures.

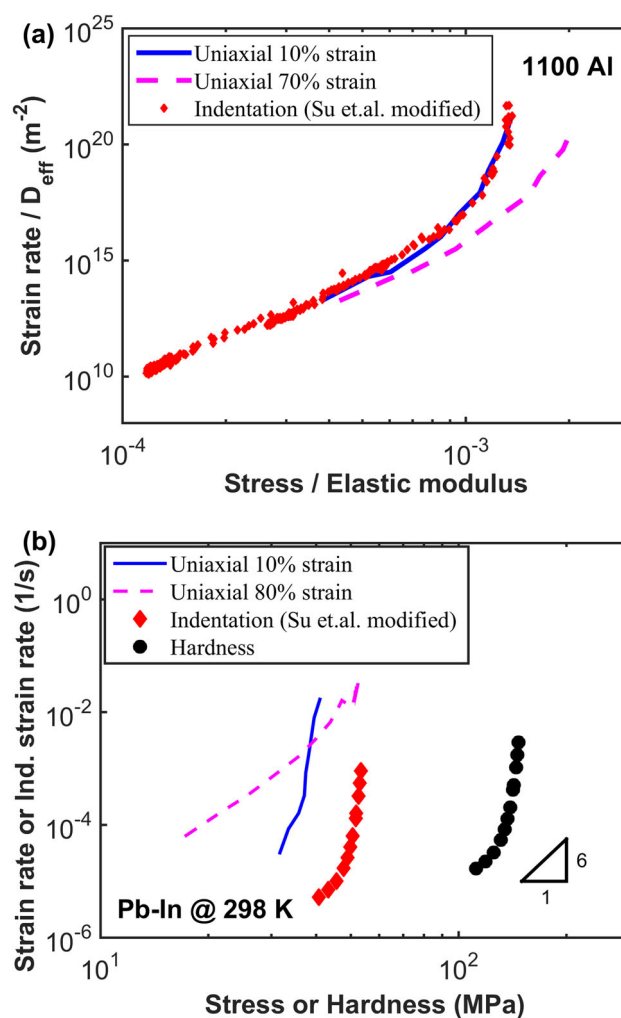


Fig. 7. Comparison of uniaxial creep data at two different values of strain and the uniaxial equivalent response determined from indentation for (a) 1100 Al from Phani and Oliver<sup>12</sup> and (b) Pb-In from Lucas.<sup>23</sup>

### SUMMARY AND CONCLUSION

The advances in high-temperature nanomechanical testing instrumentation have enabled extensive studies of indentation creep despite the experimental challenges in small-scale testing at elevated temperatures. Various methods for measuring instrumented indentation creep using geometrically self-similar indenters have been discussed along with their relative merits and demerits. While there is not one method that is a clear winner, the CLH tests have many advantages compared to the other methods, in terms of accessing a wide range of strain rates in a single experiment and minimizing the influence of depth dependent hardness effects. The accuracy of various conversion factors for determining the uniaxial creep response from indentation was assessed and Su et al.'s<sup>29</sup> conversion factors based on Bower's<sup>35</sup> theoretical analysis was found to be accurate and applicable over a wider range of stress exponents. Despite the

significant differences in the test geometry and testing methodology between the uniaxial testing and indentation testing, the uniaxial creep response determined from indentation creep testing can be remarkably close to the uniaxial response measured by traditional creep tests for materials with low stress exponents ( $\sim 1$ ) to very high stress exponents where the material response is almost strain rate independent. It is interesting to note that in the low-temperature or high-strain-rate regime, which can result in high values of the stress exponent, the stress conversion factor suggested by Su et al.<sup>29</sup> is consistent with the concept of constraint factor describing the relationship between hardness and yield strength that has been successfully applied to a wide range of materials. The representative strain of  $\sim 8\%$  induced by a Berkovich indenter may not be sufficient to achieve steady-state creep-like behavior in some cases, especially at lower temperatures. While the current methods for determining uniaxial creep response from indentation present a simple framework for steady-state, load-time history independent, power law creep, caution must be exercised in using the models within the limits of their applicability.

#### ACKNOWLEDGEMENTS

WCO and GMP's contributions to this work were supported in part by the National Science Foundation under Grant Number DMR-1427812.

#### REFERENCES

1. A.G. Atkins and D. Tabor, *J. Mech. Phys. Solids* 13, 149 (1965).
2. S. Jayaraman, G.T. Hahn, W.C. Oliver, C.A. Rubin, and P.C. Bastias, *Int. J. Solids Struct.* 35, 365 (1998).
3. A.E. Giannakopoulos and S. Suresh, *Scripta Mater.* 40, 1191 (1999).
4. M. Dao, N. Chollacoop, K.J. Van Vliet, T.A. Venkatesh, and S. Suresh, *Acta Mater.* 49, 3899 (2001).
5. M. Sakai, T. Akatsu, S. Numata, and K. Matsuda, *J. Mater. Res.* 18, 2087 (2003).
6. J.L. Bucaille, S. Stauss, E. Felder, and J. Michler, *Acta Mater.* 51, 1663 (2003).
7. S. Shim, J.-I. Jang, and G.M. Pharr, *Acta Mater.* 56, 3824 (2008).
8. L. Zhang, F. Yang, L. Sun, and Y.-H. Guo, *Chin. Rare Earths* 38, 126 (2017).
9. J. Wu, S.-B. Xue, J.-W. Wang, S. Liu, Y.-L. Han, and L.-J. Wang, *J. Mater. Sci. Mater. Electron.* 27, 12729 (2016).
10. J. Zhu, H. Xie, and Z. Liu, *Chin. J. Theor. Appl. Mech.* 45, 45 (2013).
11. J.M. Wheeler, D.E.J. Armstrong, W. Heinz, and R. Schwaiger, *Curr. Opin. Solid State Mater. Sci.* 19, 354 (2015).
12. P.S. Phani and W.C. Oliver, *Acta Mater.* 111, 31 (2016).
13. I.-C. Choi, B.-G. Yoo, Y.-J. Kim, and J. Jang, *J. Mater. Res.* 27, 3 (2012).
14. A.J. Harris, B.D. Beake, D.E.J. Armstrong, and M.I. Davies, *Exp. Mech.* 1 (2016).
15. J.C.M. Li, *Mater. Sci. Eng. A* 322, 23 (2002).
16. T.H. Hyde, K.A. Yehia, and A.A. Becker, *Int. J. Mech. Sci.* 35, 451 (1993).
17. O.D. Sherby and P.E. Armstrong, *Metall. Trans. B* 2, 3479 (1971).
18. P.M. Sargent and M.F. Ashby, *Mater. Sci. Technol.* 8, 594 (1992).
19. S. Sakai, Y. Watanabe, S. Izumi, A. Iwasaki, and T. Ogawa, *Am. Soc. Mech. Eng. Press. Vessel. Pip. Div. PVP*, 7, 301 (2005).
20. U.P. Singh and H.D. Merchant, *Metall. Trans.* 4, 2621 (1973).
21. M. Kim, K.P. Marimuthu, S. Jung, and H. Lee, *Comput. Mater. Sci.* 113, 211 (2016).
22. D. Mulhearn and T.O. Tabor, *J. Inst. Met.* 89, 7 (1960).
23. B. Lucas (Ph.D. Dissertation, University of Tennessee, Knoxville, 1997).
24. V. Maier, K. Durst, J. Mueller, B. Backes, H.W. Höppel, and M. Göken, *J. Mater. Res.* 26, 1421 (2011).
25. M.J. Mayo and W.D. Nix, *Acta Metall.* 36, 2183 (1988).
26. V. Raman and R. Berriche, *J. Mater. Res.* 7, 627 (1992).
27. G.M. Pharr, E.G. Herbert, and Y. Gao, *Annu. Rev. Mater. Res.* 40, 271 (2010).
28. P. Sudharshan Phani and W.C. Oliver, *Mater. (Basel)* 10, 663 (2017).
29. C. Su, E.G. Herbert, S. Sohn, J.A. LaManna, W.C. Oliver, and G.M. Pharr, *J. Mech. Phys. Solids* 61, 517 (2013).
30. L. Shen, W.C.D. Cheong, Y.L. Foo, and Z. Chen, *Mater. Sci. Eng. A* 532, 505 (2012).
31. N.J. Martinez and Y.-L. Shen, *J. Mater. Eng. Perform.* 25, 1109 (2016).
32. J. Dean, J. Campbell, G. Aldrich-Smith, and T.W. Clyne, *Acta Mater.* 80, 56 (2014).
33. R. Goodall and T.W. Clyne, *Acta Mater.* 54, 5489 (2006).
34. V. Maier, B. Merle, M. Göken, and K. Durst, *J. Mater. Res.* 28, 1177 (2013).
35. A.F. Bower, N.A. Fleck, A. Needleman, and N. Ogbonna, *Proc. R. Soc. London. Ser. A Math. Phys. Sci.* 441, 97 (1993).
36. H. Takagi, M. Dao, M. Fujiwara, and M. Otsuka, *Philos. Mag.* 83, 3959 (2003).
37. H. Takagi, M. Dao, and M. Fujiwara, *Mater. Trans.* 55, 275 (2014).
38. N.Q. Chinh and P. Szommer, *Mater. Sci. Eng. A* 611, 333 (2014).
39. H. Takagi and M. Fujiwara, *Mater. Sci. Eng. A* 602, 98 (2014).
40. S. Fujisawa, A. Yonezu, M. Noda, and B. Xu, *J. Eng. Mater. Technol.* 139, 21004 (2017).
41. M.E. Cordova and Y.-L. Shen, *J. Mater. Sci.* 50, 1394 (2016).
42. Y.-T. Cheng and C.-M. Cheng, *Philos. Mag. Lett.* 81, 9 (2001).
43. V.M.F. Marques, B. Wunderle, C. Johnston, and P.S. Grant, *Acta Mater.* 61, 2471 (2013).
44. A.A. Elmustafa, S. Kose, and D.S. Stone, *J. Mater. Res.* 22, 926 (2007).
45. H. Oikawa, H. Sato, and K. Maruyama, *Mater. Sci. Eng.* 75, 21 (1985).
46. Z. Tobolová and J. Čadek, *Philos. Mag.* 26, 1419 (1972).
47. I.S. Servi and N.J. Grant, *Trans. AIME* 191, 909 (1951).
48. T. Altan and F.W. Boulger, *J. Eng. Ind.* 95, 1009 (1973).
49. B.N. Lucas and W.C. Oliver, *Metall. Mater. Trans. A* 30, 601 (1999).
50. O.D. Sherby, R.H. Klundt, and A.K. Miller, *Metall. Trans. A* 8, 843 (1977).